30th International Congress on Sound and Vibration

ICSV30 AMSTERDAM 8-11 JULY 2024

THE EFFECT OF TRACKING RESOLUTION ON THE STABILITY OF A HEADTRACKER EQUIPPED ACTIVE HEADREST NOISE CONTROL SYSTEM

Chung Kwan Lai, Jordan Cheer, Chuang Shi

University of Southampton, Institute of Sound and Vibration Research, Highfield, Southampton, United Kingdom.
E-mail: c.k.lai@soton.ac.uk

Previous research has shown that by utilising headtracking to update the head position and the corresponding plant responses in an active noise cancelling headrest application improves the performance of the controller. Although it is desirable for the headtracker to track the users head as accurately as possible, there is a trade-off to be paid in the complexity of the calibration process when utilising a large number of plant responses. This paper presents an investigation into the effect of tracking resolution for a local active noise control system operating in the presence of head movements. It is shown, through numerical simulations, that increasing the tracking resolution increases the upper frequency of stable control performance. It is also shown that the tracking resolution is more sensitive for some geometrical regions than others, which may inform the design of an efficient headtracking calibration procedure.

Keywords: Local active sound control, Active headrest system, Headtracking

1. Introduction

The integration of headtracking into local active noise control systems, which aim to create a local zone of quiet around the user's ears [1], has recently gained significant research interest particularly for application to active headrest systems [2]. The headtracker is used to update the plant model used in the control system based on the current head position, thus reducing the mismatch between the plant model and the true plant response. This results in an improvement in the control performance and stability with respect to head movements. Many studies have been conducted to further understand and improve the performance of headtracker equipped active control systems, and these can be categorized as either understanding the variation in the plant response under head movement [3], improving the tracking capability [4, 5], or making the control system more robust towards headtracking limitations [6]. While it is ideal for the headtracker to update the plant model to approximate the true plant response as accurately as possible, such an approach may not be feasible in practice, as this would require a lengthy calibration process to measure the plant responses for many head positions. Additionally, the tracking accuracy may also be limited by the headtracker's hardware, where limited accuracy could degrade the control stability even under a head-tracked configuration. This paper, while assuming that the error signals at the ears are perfectly known thus neglecting the effect of virtual sensing inaccuracies due to head movement,

shall investigate the control stability of a headtracker equipped local active control system under different tracking resolutions. Section 2 will outline the geometrical arrangement used for the active headrest system and the range of possible head movements considered. This is followed by an examination of the control stability due to varying tracking resolutions for the different types of head movements in Section 3 – Section 5, and finally conclusions are presented in Section 6.

2. Active headrest setup configuration

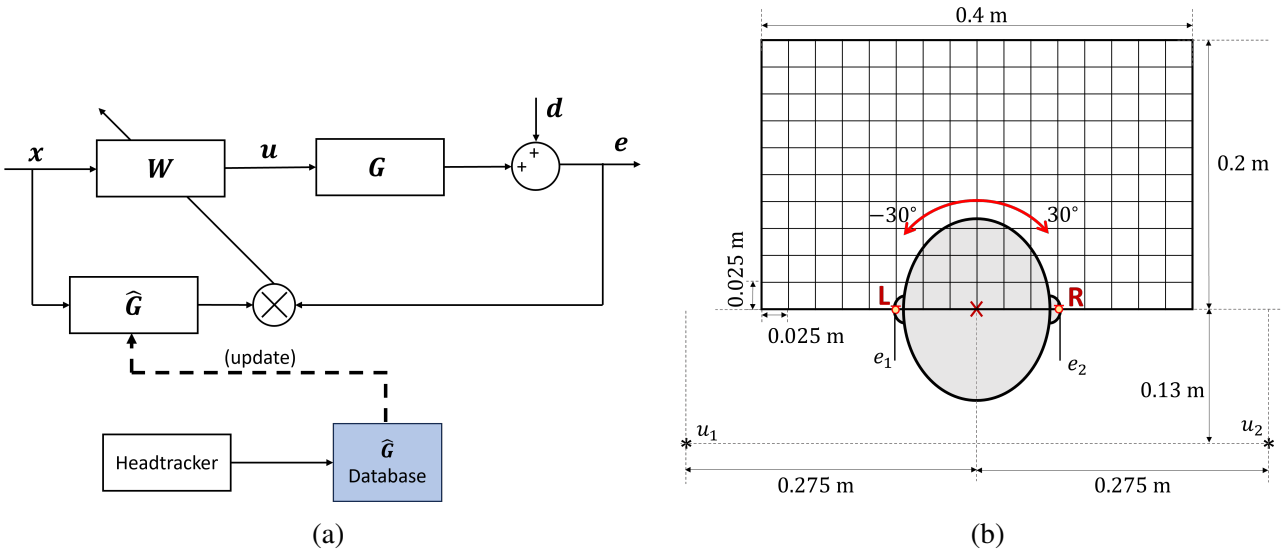

(a) (b)

Figure 1: The (a): block diagram of the multichannel feedforward active control system and (b): configuration for the active headrest where the head translates in the horizontal (left/right) and vertical (front/back) direction within a (0.4 m $\times$ 0.2 m) translational grid, and rotates within a $-30°$ to $+30°$ rotational grid. The minimum grid spacings for the translational and rotational grid were given by 0.025 m and $10°$ respectively.

Figure 1 presents the numerically simulated configuration for the active headrest, which utilizes a boundary element model of the KU100 head [7] implemented in COMSOL, which represent the user's head, and two monopole point sources with control signals u_1 and u_2 that represent the secondary sources in the active headrest. The plant responses from the secondary sources to the error sensors are denoted as $\mathbf{G}$. During the initial calibration phase, the plant responses for each head position within a discrete translational grid of (0.4 m $\times$ 0.2 m) and a discrete rotational grid ranging from $-30°$ to $30°$ were calculated and were later used to update the plant model, as denoted by $\hat{\mathbf{G}}$, based on the head position provided by the headtracker.

Due to the resolution imposed by the plant response measurement calibration phase, the control system can only update the plant model when the head moves between the points defined by the grid. This implies that as the head moves from one position to another while within the resolution of the grid, a mismatch may arise between the actual plant response and the current plant model employed in the control system. Such a discrepancy could potentially induce instability within the control system, particularly for coarse grid resolutions. Assuming a tonal disturbance, the stability condition when the control system adapts through the steepest gradient descent method [8] is given by

$$\mathrm{Re}\left\{\mathrm{eig}\left[\hat{\mathbf{G}}^{\mathrm{H}}\mathbf{G}\right]\right\} > 0, \tag{1}$$

where the superscript 'H' denotes the Hermitian transpose of the matrix, and eig $[\cdot]$ and Re $\{\cdot\}$ denote the eigenvalue and the real operator, respectively. We shall classify the change in head movements into three separate groups, as shown in Figure 2. In each ease, the graphics showed a few instances of the range of possible head movements within the line grid defined in Figure 1b, for which the plant model for the original head position, indicated by the red cross, is still used.

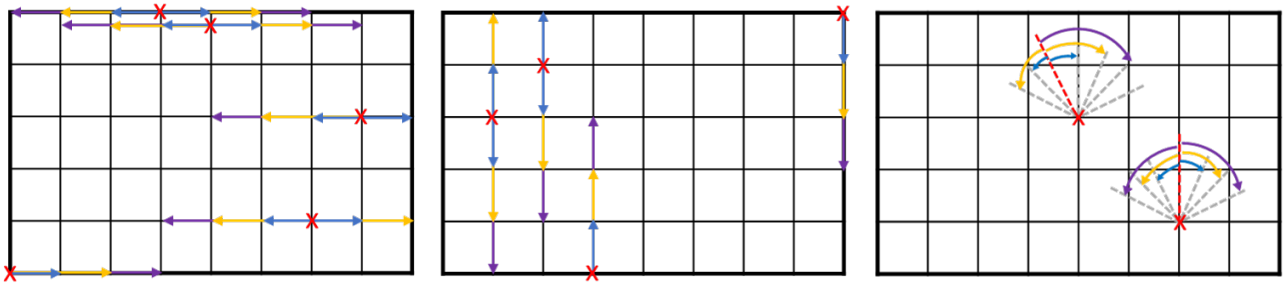

(a) (b) (c)

Figure 2: The potential set of head movements due to (a): horizontal head translation (left/right), (b): vertical head translation (front/back) and (c): head rotation under different grid resolutions. The head orientation was fixed at $0°$ for the translational case.

3. Effect of horizontal head translation on control stability

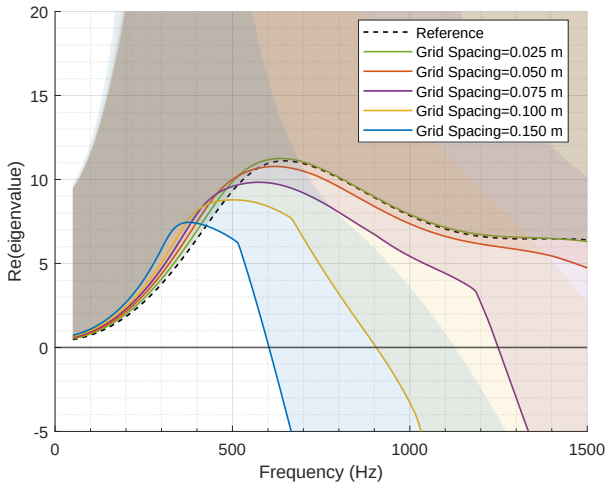

Figure 3: The set of eigenvalues due to a combination of horizontal head movements for a head rotation of $0°$. The line plots represent the smallest eigenvalue among all head movements, and the shaded region represents the range of eigenvalues for all head movements.

Figure 3 shows the set of smallest eigenvalues obtained from Equation 1 for each possible horizontal head movement as illustrated in Figure 2a. From these results it can be seen that as the grid resolution decreases at a fixed head rotation of $0°$, the frequency at which an eigenvalue turns negative decreases. This implies that with a decrease in grid resolution, the frequency at which system instability occurs decreases. However, the control instability for this frequency only applies to a certain set of head movements, as indicated by the shaded regions that represent the range of potential head movements at various positions, which contain positive eigenvalues. As frequency increases, an increasing portion of the shaded region

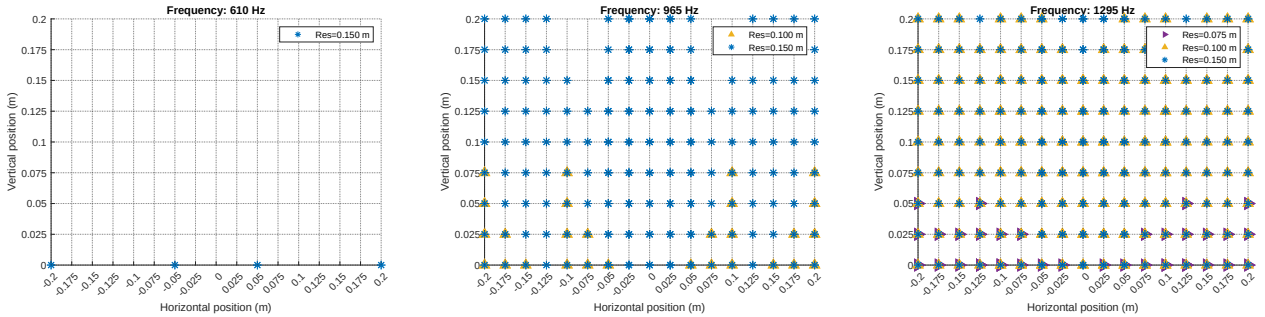

Figure 4: The location of horizontal head movements where instability occurs in terms of the horizontal and vertical grid points. Each graphic illustrates a specific frequency at which instability first arises for one of the grid resolutions.

turns negative, suggesting that an increasing number of head movements lead to control instability. This can be verified in Figure 4, which pinpoints the geometric position of the head when control instability based on horizontal head movements start to occur. It is also interesting to note that the positions where the system becomes unstable due to horizontal head movement first occur at the positions closest to the secondary sources, and then extends away from the secondary sources as the frequency increases. This trend is similar across different grid spacings, which in turn allows us to predict the possible location where the control system becomes unstable. For the 0.025 m and 0.05 m grid spacings, it can be seen that the control system remains stable throughout the entire frequency range and closer to the reference case where no head movement occurs.

4. Effect of vertical head translation on control stability

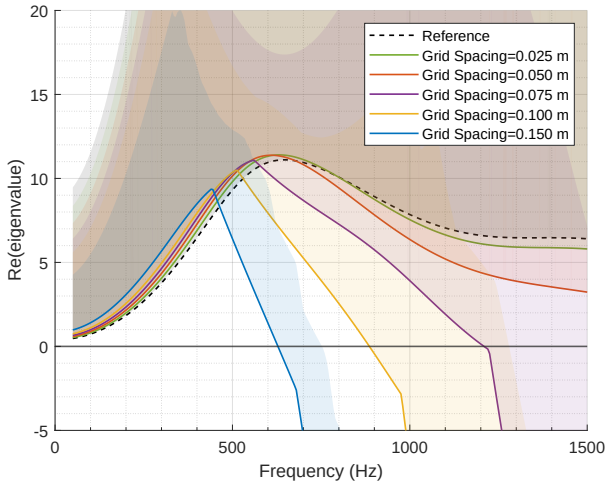

Figure 5: The set of eigenvalues due to a combination of vertical head movements for a head rotation of $0°$. The line plots represent the smallest eigenvalue among all head movements, and the shaded region represents the range of eigenvalues for all head movements.

When the head moves vertically within the bands of the different grid resolutions defined in Figure 2b, the eigenvalue plot for all possible combinations of head movement is shown in Figure 5. These results show similar trends to those observed in Figure 3, where an increase in grid spacing results in a reduction in the upper frequency limit for control stability. However, it can also be observed that the shaded region

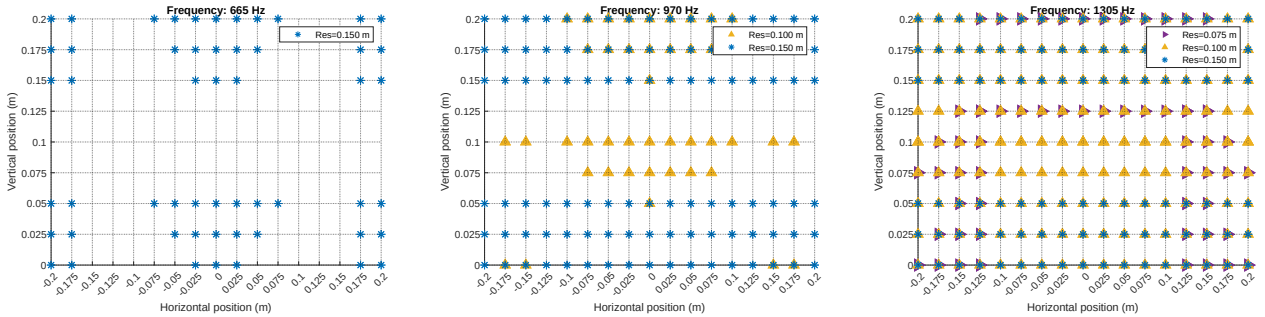

Figure 6: The location of vertical head movements where instability occurs in terms of its horizontal and vertical grid points. Each graphic illustrates a specific frequency at which instability first arises for one of the grid resolutions.

in Figure 5, in particular for the grid spacings of 0.15 m and 0.1 m, is much narrower compared to the horizontal head translation case in Figure 3. This implies that the combination of vertical head movements result in control instability within a much more limited frequency range, compared to the horizontal head movement shown in Figure 3.

The position at which the control system becomes unstable due to vertical head movement for different frequencies is shown in Figure 6 to vary for different grid resolutions. At the frequency where the 0.15 m grid spacing becomes unstable, system instability occurs at horizontal positions of 0 m and ± 0.2 m in the first instance. The grid spacings of 0.1 m and 0.075 m, however, do not follow the same trend as observed in the 0.15 m case, and instability occurs first at the top center and the bottom corners of the grid respectively. For the 0.05 m and 0.025 m case, on the other hand, the control system remains stable throughout the frequency range, and this is similar to the horizontal head movements in Figure 3.

5. Effect of head rotation on control stability

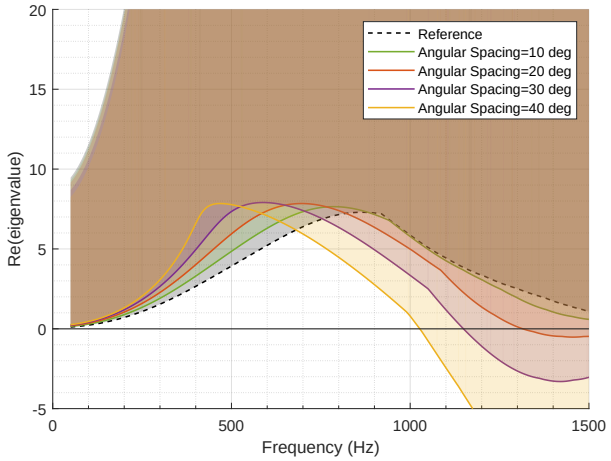

Figure 7: The set of eigenvalues due to a combination of head rotation for each translational grid points. The line plots represent the smallest eigenvalue among all head movements, and the shaded region represents the range of eigenvalues for all head movements.

When the head is subject to rotation, the eigenvalue plot is shown in Figure 7 and this shows a similar trend to the translational cases, where increasing the angular spacing decreases the upper frequency limit

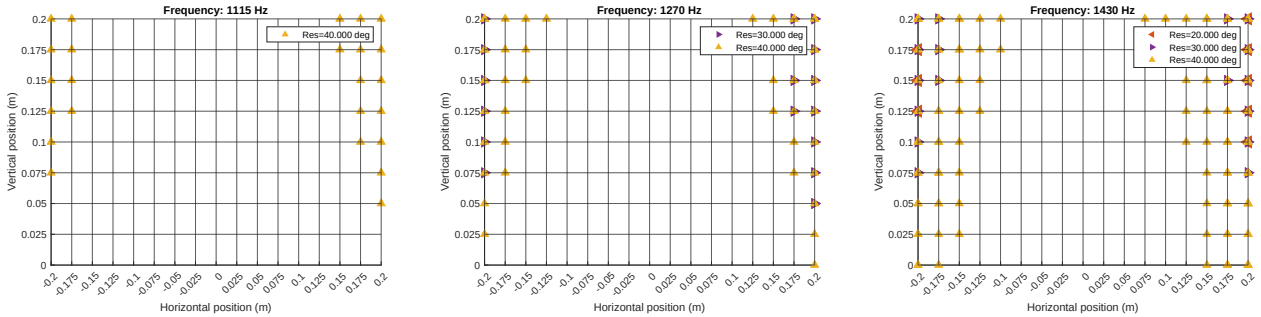

Figure 8: The location of head rotations where instability occurs in terms of the horizontal and vertical grid points. Each graphic illustrates a specific frequency at which instability first arises for one of the grid resolutions.

for control stability. From the results, only a 10° rotational spacing ensures control stability throughout the frequency range. Examining the location where instability initially occurs in Figure 8, we observe that control instability emerges first at the translational grid positions of $(\pm 0.2, +0.2)$ m. As the frequency increases, this instability zone extends closer to the source. Interestingly, this behavior remains consistent across different angular resolutions.

6. Conclusions

Although control instability caused by head movements for an active headrest system can be improved with the use of headtracking, having a low grid resolution can affect the overall control stability at higher frequencies. Numerical simulations have shown that decreasing the grid resolution reduces the upper frequency limit where the control system remains stable. This insight allows the optimal grid resolution to be chosen to ensure stability over a desired frequency range, while minimising the calibration complexity required in terms of the number of plant responses that must be measured.

Coincidentally, the position at which the control system first becomes unstable exhibits a distinct trend among different grid positions. While the position of control instability due to horizontal head translation and head rotation are consistent with various grid resolutions, the position where the control system becomes unstable due to vertical head translation differs for different grid resolutions. Further research is needed to fully understand this phenomenon and its implications for the design and operation of active headrest systems.

7. Acknowledgments

The work was supported by the project IN-NOVA: Active reduction of noise transmitted into and from enclosures through encapsulated structures, which has received funding from the European Unions Horizon Europe programme under the Marie Sklodowska-Curie grant agreement no. 101073037. This work was funded by UK Research and Innovation under the UK government's Horizon Europe funding guarantee [grant number EP/X027767/1].

REFERENCES

1. Olson, H. F. and May, E. G. Electronic Sound Absorber, **25** (6), 1130–1136.

2. Elliott, S. J., Jung, W. and Cheer, J. Head tracking extends local active control of broadband sound to higher frequencies, **8** (1), 5403.

3. Yang, Z., Wang, Y. and Tao, J. Variation of the secondary acoustic paths from loudspeakers at the seat shoulder in an automobile cabin, *INTER-NOISE and NOISE-CON Congress and Conference Proceedings*.

4. Li, H., Chen, K., Tao, J. and Qiu, X. Using infrared radars for ear positioning in active noise control headrests, *INTER-NOISE and NOISE-CON Congress and Conference Proceedings*.

5. Liu, Y., Li, H., Zou, H., Lu, J. and Lin, Z., (2023), *Active Headrest Combined with a Depth Camera-Based Ear-Positioning System*.

6. Chen, H., Huang, X., Zou, H. and Lu, J. Research on the Robustness of Active Headrest with Virtual Microphones to Human Head Rotation, **12** (22), 11506.

7. Di Giusto, F., Van Ophem, S., Desmet, W. and Deckers, E. Analysis of laser scanning and photogrammetric scanning accuracy on the numerical determination of Head-Related Transfer Functions of a dummy head, *Acta Acustica*, **7**, 53, (2023).

8. Elliott, S., *Signal Processing for Active Control*, Academic Press (2000).